

Freeform Rigid-Foldable Structure using Bidirectionally Flat-Foldable Planar Quadrilateral Mesh

Tomohiro Tachi

The University of Tokyo

Abstract. *This paper presents a computational design method to obtain collapsible variations of rigid-foldable surfaces, i.e., continuously and finitely transformable polyhedral surfaces, homeomorphic to disks and cylinders. Two novel techniques are proposed to design such surfaces: a technique for obtaining a freeform variation of a rigid-foldable and bidirectionally flat-foldable disk surface, which is a hybrid of generalized Miura-ori and eggbox patterns, and a technique to generalize the geometry of cylindrical surface using bidirectionally flat-foldable planar quadrilateral mesh by introducing additional constraints to keep the topology maintained throughout the continuous transformation. Proposed methods produce freeform variations of rigid-foldable structures that have not been realized thus far. Such a structure forms a one-DOF mechanism with two possible flat states. This enables the designs of deployable structures useful for packaging the boundary of architectural spaces, space structures, and so on.*

1 Introduction

A polyhedral surface composed of rigid facets connected by rotational edges forms a kinetic mechanism: a rigid folding mechanism. Several collapsible structures are proposed using this type of kinetic mechanism, such as Miura-ori [Miura 1980] and eggbox patterns [Brunner 1965] (Figure 1). Such a rigid-foldable and flat-foldable surface is useful as a deployable and transformable structures in an architectural context because of the following advantages.

1. The existence of a collapsed state enables compact packaging of the structure.
2. The synchronized complex folding motion produced by constrained rotational hinges can be controlled with simple manipulation.
3. The transformation mechanism that does not rely on the flexibility of materials can be made out of thick rigid panels and hinges.
4. The watertightness of the surface maintained throughout the transformation is potentially suitable for the envelope of a space, a partition, and the facade of a building.

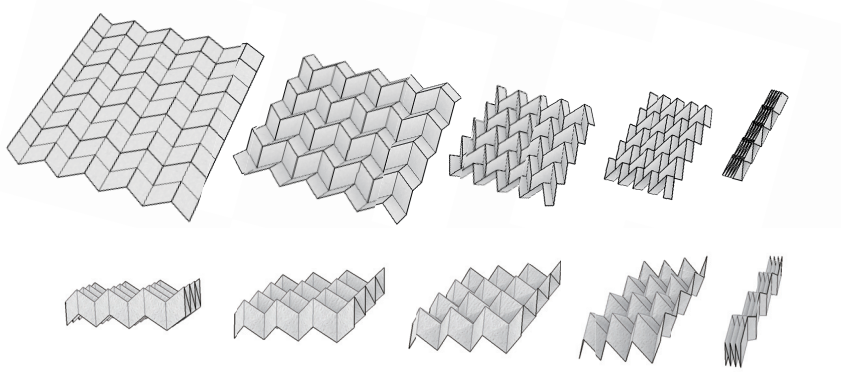


Figure 1: Folding motions of Miura-ori (Top) and eggbox pattern (Bottom).

In order to apply such kinetic surfaces to design purposes, it is required that we can control the three-dimensional shape of the surface and its behavior so that they are consistent with the design requirements. Design requirements in architectural context include environmental conditions, functional requirements, configuration of surrounding buildings and structures, and user's preference. However, since the rigid-foldability of known surfaces strongly relies on the symmetry of the pattern, designing such structures could not be done in an ad-hoc approach; the geometric constraints must be generally investigated to solve an inverse problem of obtaining a pattern from the resulting form and behavior. The objective of our study is thus to freely design kinetic forms using design methods based on computational geometry.

As the first step to achieve this goal, the author proposed a freeform design method of kinetic structures based on origami (developable surface) to provide design variations of Miura-ori through an interactive design system in which a user can deform the surface freely while sustaining the rigid-foldability of the surface ([Tachi 2009a]). This method yields variations of rigid-foldable origami models that have never been achieved otherwise, however, the method was not general enough for design applications, especially of architecture, since the developability condition used is not always an essential condition when we construct structures from multiple parts. In particular, this developability condition disables the design of rigid-foldable collapsible cylinders, realization of which can contribute the designs of surrounding of a volume of a space, collapsible containers, compound surface structures, and so on. This limitation mainly comes from the fact that a cylindrical surface cannot have a globally developed state under the conventional definition.

This paper provides a novel method that enables a freeform variation of such rigid-foldable structure, not restricted by the developability of the surface or the disk topology. We will solve this design problem by extending and combining the ideas of generalized Miura-ori [Tachi 2009a] (or flat-foldable 4-valent-vertex origami)

and generalized eggbox pattern (or discrete Voss surface) [Schief et al. 2007] to produce bidirectionally flat-foldable planar quadrilateral mesh. Such a mesh has nice generalized characteristics: it is bidirectionally flat-foldable and produces one-DOF mechanism. Required design condition is loose compared to purely developable surface and it allows asymmetric and cylindrical variations. We will show a novel design method to obtain rigid-foldable collapsible cylinders by deforming symmetric rigid-foldable cylinders of [Tachi 2009b] into asymmetric ones.

2 Geometry of Rigid-Foldable Quadrilateral Mesh Disk

This section shows the geometry of 4-valency rigid-foldable mesh with two flat states that combines flat-foldable origami surface and discrete Voss surface. A 4-valency mesh or a quadrilateral-mesh surface in general does not enable a continuous rigid-folding motion because an overconstrained system is constructed. This is because the configuration of a rigid-foldable structure homeomorphic to a disk can be represented by the folding angles of edges, while these variables are constrained at each vertex by 3 equations as it is used in the simulation of rigid origami [Tachi 2009c]; if we are to construct a quadrilateral mesh, then the number of constraints exceeds the number of variables only by making 3×3 array. However, Miura-ori [Miura 1980] and eggbox patterns [Brunner 1965] are known to produce singular one-DOF mechanisms (Figure 1) because of their redundant constraints. Miura-ori is a flat-foldable origami surface composed of parallelograms used for packaging of large membranes in the space. The surface produces a synchronized kinetic motion of expanding in x and y directions at the same time from a collapsed state to a completely developed state (Figure 1 Top). Eggbox pattern is a polyhedral surface similarly composed of parallelograms but is not a developable surface. This has two flat-folded states and produces a different one-DOF kinetic behavior from that of Miura-ori; the surface expands in x direction when it collapses in y direction (Figure 1 Bottom). While Miura-ori is a surface with foldlines folded at the same time, eggbox pattern is a surface that has two groups of foldlines collapsed at the same time.

Since Miura-ori and eggbox patterns are surfaces composed of congruent parallelograms, the redundancy of constraints required for the mechanism seem to originate in its global repeating symmetry. However, the condition to produce such redundancy actually is a result of its intrinsic symmetry, i.e., the angles coincidence at each vertex, which also contribute to bi-directional flat-foldability of the surfaces (Miura-ori is developable and flat-foldable. eggbox pattern is flat-foldable in two directions). The intrinsic symmetries of Miura-ori and eggbox pattern, yield generalized forms of rigid-foldable origami surface [Tachi 2009a] and discrete Voss surface [Schief et al. 2007], respectively. In addition, these surfaces can be merged into one generalized hybrid surface, i.e., bidirectionally flat-foldable planar quadrilateral mesh, based on the fact that the behaviors of the two surfaces can be represented using a common form.

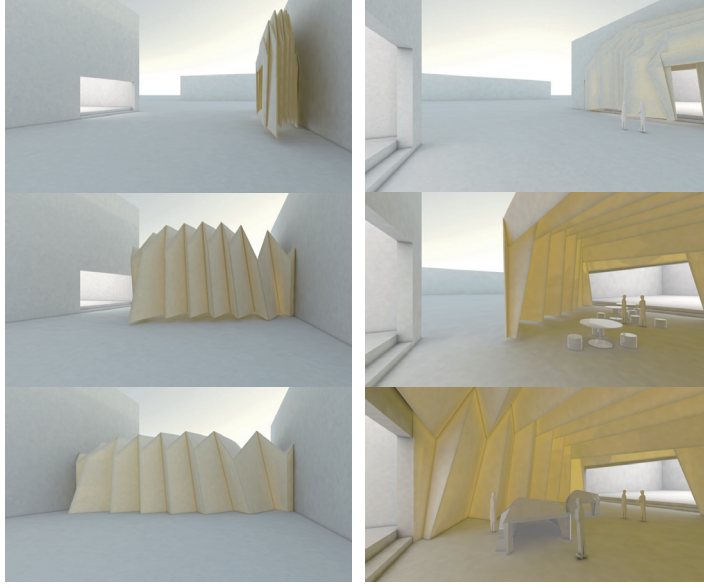


Figure 2: A corrugated vault used as a transformable architecture that connects two existing buildings.

2.1 Generalized Miura-ori

The rigid-foldability condition of generalized Miura-ori is presented by [Tachi 2009a]: consider a planar quad mesh surface of disk topology whose vertices are incident to 4 foldlines; when the surface is developable and flat-foldable, finite rigid-foldability of the surface is equivalent to the existence of one valid semi-folded state. This sufficient condition for rigid-foldability yields rigid-foldable generalization of Miura-ori. The condition also applies to any other degree-4 vertex based patterns such as asymmetric vault pattern shown in Figure 2.

The behavior of the surface is represented by the configuration of fold angles. A vertex with 4 foldlines, and thus with 4 sector angles $\theta_i (i = 0, 1, 2, 3)$, form a one-DOF mechanism (Figure 3 Top). In the case of developable and flat-foldable surface, condition of origami (i.e., developability) and flat-foldability given by $\sum_{i=0}^3 \theta_i = 2\pi$ and $\sum_{i=0}^3 (-1)^i \theta_i = 0$, respectively, force the sector angles to satisfy

$$\theta_0 = \pi - \theta_2 \quad \text{and} \quad \theta_1 = \pi - \theta_3. \quad (1)$$

According to [Tachi 2009a], the fold angles ρ_i and ρ_j incident to the vertex are related as follows:

$$\tan \frac{\rho_i}{2} = \begin{cases} A_{i,j} \tan \frac{\rho_j}{2} & (i - j = 1 \text{ or } 3 \pmod{4}) \\ \pm \tan \frac{\rho_j}{2} & (i - j = 2 \pmod{4}) \end{cases} \quad (2)$$

where the latter represents that pairs of opposite foldlines have an equal absolute folding angles, and $A_{i,j}$ is the coefficient between these two equivalent pairs determined by $\theta_0, \dots, \theta_3$, i.e., intrinsic measure in the crease pattern independent from the folding angles. Specifically, if $|\rho_0| = |\rho_2| > |\rho_1| = |\rho_3|$,

$$|A_{0,1}| = \sqrt{\frac{1 + \cos(\theta_0 - \theta_1)}{1 + \cos(\theta_0 + \theta_1)}}.$$

Note that this relationship is a special case of the generalized form of origami vertex presented by [Huffman 1976].

This gives an explicit configuration of folding angles of all foldlines globally connected via degree-4 vertices:

$$\left\{ \tan \frac{\rho_i(t)}{2} \right\} = \left\{ \tan \frac{\rho_i(t_0)}{2} \right\} \frac{\tan \frac{t}{2}}{\tan \frac{t_0}{2}}, \quad (3)$$

where t ($0 \leq t \leq \pi$) is the parameter that defines the folding amount ($t = 0$ and $t = \pi$ indicate developed and flat-folded states respectively) and $\left\{ \tan \frac{\rho_i(t_0)}{2} \right\}$ is an arbitrary semi-folded state ($0 < t_0 < \pi$). Generalized Miura-ori thus shows a kinetic motion of expanding in x and y directions at the same time.

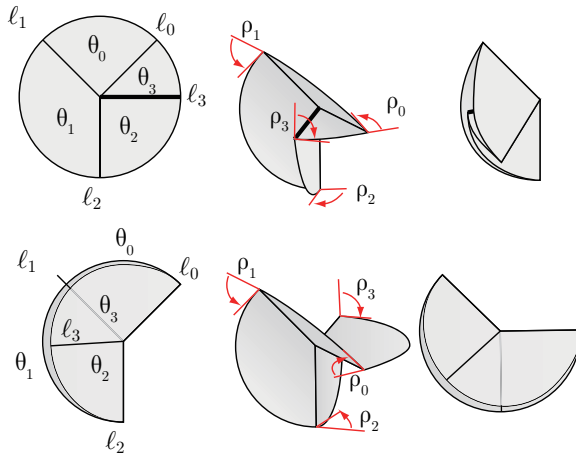


Figure 3: The folding motions of vertices of origami (Top) and discrete Voss surface (Bottom). Note that set of planes used is identical.

2.2 Generalized Eggbox Pattern

Eggbox pattern can be generalized as a discrete Voss surface; the rigid-foldability of discrete Voss surface is proved by [Schief et al. 2007]. Even though the term discrete Voss surface implies a mesh pattern that represents a smooth surface, corrugated surfaces such as eggbox pattern is also included in the family, since it is defined by the intrinsic angular condition that the opposite angles are equal. Every interior

vertex on a discrete Voss surface is incident to 4 edges (or foldlines) and sector angles θ_i ($i = 0, 1, 2, 3$) that satisfy the following:

$$\theta_0 = \theta_2 \quad \text{and} \quad \theta_1 = \theta_3. \quad (4)$$

Note the similarity to (1): in fact, the set of planes that form an origami vertex and eggbox vertex are identical (Figure 3). According to [Schief et al. 2007], the folding angles ρ_i and ρ_j are similarly written as the following form:

$$\tan \frac{\rho_i}{2} = \begin{cases} A_{i,j} \cot \frac{\rho_j}{2} & (i-j = 1 \text{ or } 3 \pmod{4}) \\ \tan \frac{\rho_j}{2} & (i-j = 2 \pmod{4}). \end{cases}$$

If we measure the folding angles of one of the opposite pairs by their complementary angles $\rho'_i = \pi - \rho_i$, this becomes

$$\tan \frac{\rho_i}{2} = \begin{cases} A_{i,j} \tan \frac{\rho'_j}{2} & (i-j = 1 \text{ or } 3 \pmod{4}) \\ \tan \frac{\rho'_j}{2} & (i-j = 2 \pmod{4}). \end{cases} \quad (5)$$

Therefore the kinematics of Miura-ori and discrete Voss surface are essentially identical as represented by Equation (3).

2.3 Hybrid Surface: Bidirectionally Flat-foldable Planar Quadrilateral Mesh

Here, we introduce a new type of functional patterns, i.e., BDFFPQ mesh (defined later), based on combining the geometry of origami and discrete-Voss surface. We introduce the concept of *complementary foldlines*, which are edges whose folding angles are measured by their complementary angles, thus a complementary foldline folds from $\pm\pi$ to 0 when an ordinary foldline folds from 0 to $\pm\pi$. By using complementary foldlines (CFLs) along with foldlines (FLs), we can produce a 4-valency network that consistently joins the vertices of origami and discrete Voss surfaces, so that one-DOF kinetic motion exists.

In order to understand this behavior, we define extended “developed state” and “flat-folded state” as follows:

Developed state: A flat state in which every edge has rotational angle of 0 (thus foldlines are unfolded and complementary foldlines are folded).

Flat-folded state: A flat state in which every edge has rotational angle of $\pm\pi$ (the sign shows mountain or valley).

Here, notice that complementary foldlines and foldlines are interchangeable by calling a developed state a flat-folded state and vice versa.

Here we define *bidirectionally flat-foldable planar quadrilateral mesh (BDFFPQ mesh)* a 4-valency network mesh surface that follows the following conditions.

- The surface is polyhedral, i.e., composed of planar facets, and every edge is either FL or CFL.

- The surface has developed and flat-folded states, where the intersection of the overlapped facets is ignored.
- Each interior vertex's incident edges are either 4 FLs, 4 CFLs, or 2 FLs + 2CFLs in which a pair of CFLs or FLs is an opposite pair.

Rigid foldability of such a surface is represented as follows when the surface is homeomorphic to a disk.

Theorem 1 *If and only if BDFFPQ mesh homeomorphic to a disk with more than one interior vertex has one intermediate folded state, the surface is finitely rigid-foldable.*

Proof: Rigid-foldability of a polyhedral disk surface can be represented by the existence of a continuous solution in the configuration space. From the developability and flat-foldability condition, it follows that subnetwork composed of only FLs (CFLs) must divide the surface completely into one or multiple regions each of which is assigned with either +1 or -1 such that the signs of adjacent regions are opposite. The sign indicates the orientation of facet in the flat-folded (developed) state. Then the developability and flat-foldability of the network for each vertex is represented as follows:

$$\text{developability: } \begin{cases} \sum_{i=0}^3 \sigma^{\text{dev}}(i)\theta_i = 0 & \text{for 4CFL or 2FL + 2CFL vertex} \\ \sum_{i=0}^3 \theta_i = 2\pi & \text{for 4FL vertex,} \end{cases} \quad (6)$$

$$\text{flat-foldability: } \begin{cases} \sum_{i=0}^3 \sigma^{\text{ff}}(i)\theta_i = 0 & \text{for 4FL or 2FL + 2CFL vertex} \\ \sum_{i=0}^3 \theta_i = 2\pi & \text{for 4CFL vertex,} \end{cases} \quad (7)$$

where $\sigma^{\text{dev}}(i)$ and $\sigma^{\text{ff}}(i)$ indicate the assigned signs of the facet incident to the sector angle i in the developed and flat-folded states respectively.

A 2FL+2CFL vertex satisfies $\sum_{i=0}^3 \sigma(i)\theta_i = 0$ for both σ in developed and flat-folded states ($\{\sigma(0), \sigma(1), \sigma(2), \sigma(3)\} = \{1, 1, -1, -1\}$ and $\{1, -1, -1, 1\}$); therefore $\theta_0 = \theta_2$ and $\theta_1 = \theta_3$. Hence, the vertex is a discrete Voss vertex and the folding motion follows (5). A 4FL or 4 CFL vertex is essentially a vertex of Miura-ori and the folding angles of incident edges follow the kinetic motion represented by (3). Since we represent the folding angles of complementary foldlines by their complementary angles, these relations can be represented in the following single form:

$$\tan \frac{\rho_i}{2} = A'_{i,j} \tan \frac{\rho_j}{2},$$

where $A'_{i,j} = 1/A_{i,j}$ for 4CFL vertices. Since all the foldlines are connected to each other, the transformation follows (3). Therefore if and only if there exists one intermediate configuration $\left\{ \tan \frac{\rho_i(t_0)}{2} \right\}$, there exists a continuous valid configurations $\left\{ \tan \frac{\rho_i(t)}{2} \right\}$. \square

3 Design Variations of Rigid Foldable Surface

For obtaining design variations, we adopt the perturbation based approach used in [Tachi 2009a]. We first obtain a valid existing BDFFPQ mesh in a flat state; this can be done quite easily, e.g., by using a square grid and assigning mountain, valley, complementary mountain, and complementary valley to the edges. Here, we can roughly design the kinetic behavior since an origami vertex tries to expand the surface in two directions at the same time, while a discrete Voss vertex tries to expand in one direction while collapsing in the other direction.

Then we deform the pattern while sustaining the developability and flat-foldability conditions. The configuration of the mesh surface is represented by the coordinates of vertices \mathbf{x} forming a triangular mesh whose edges are either triangulation edges or complementary or ordinary foldlines. This triangular mesh satisfies the planarity condition for each facet and flat-foldability (7) and developability (6) conditions for each interior vertex. Thus an infinitesimal deformation of mesh configuration must satisfy:

$$\mathbf{c}(\mathbf{x}) = \begin{bmatrix} \mathbf{c}^{\text{dev}}(\mathbf{x}) \\ \mathbf{c}^{\text{ff}}(\mathbf{x}) \\ \mathbf{c}^{\text{planar}}(\mathbf{x}) \end{bmatrix} = \mathbf{0}, \quad (8)$$

where $\mathbf{c}^{\text{dev}}(\mathbf{x})$ is a N^{Vint} -vector (N^{Vint} is the number of interior vertices) whose element is

$$\begin{cases} \sum_{i=0}^3 \sigma^{\text{dev}}(i)\theta_i & \text{for 4CFL or 2FL + 2CFL vertex} \\ 2\pi - \sum_{i=0}^3 \theta_i & \text{for 4FL vertex,} \end{cases}$$

$\mathbf{c}^{\text{ff}}(\mathbf{x})$ is a N^{Vint} -vector whose element is

$$\begin{cases} \sum_{i=0}^3 \sigma^{\text{ff}}(i)\theta_i & \text{for 4FL or 2FL + 2CFL vertex} \\ 2\pi - \sum_{i=0}^3 \theta_i & \text{for 4CFL vertex,} \end{cases}$$

and $\mathbf{c}^{\text{planar}}(\mathbf{x})$ is a vector with dimension of the number of triangulating edges, and its element is its corresponding folding angle ρ_i .

Since the number of variables exceeds the number of constraints for a quadrilateral mesh structure with multiple boundary edges, the Jacobian matrix of the constraint $\left[\frac{\partial \mathbf{c}}{\partial \mathbf{x}} \right]$ is a rectangular matrix whose number of columns exceeds the number of rows. An infinitesimal solution space of this constraint can be calculated as:

$$\Delta \mathbf{x} = \left(\mathbf{I} - \left[\frac{\partial \mathbf{c}}{\partial \mathbf{x}} \right]^+ \left[\frac{\partial \mathbf{c}}{\partial \mathbf{x}} \right] \right) \Delta \mathbf{x}_0, \quad (9)$$

where $\left[\frac{\partial \mathbf{c}}{\partial \mathbf{x}} \right]^+$ is the pseudo-inverse (Moore-Penrose generalized inverse) of the Jacobian matrix, and $\Delta \mathbf{x}_0$ represents an arbitrary vector. Equation (9) calculates the valid perturbation closest to $\Delta \mathbf{x}_0$ by orthogonal projection to the solution space; therefore,

the user input such as the drag motion of vertices through GUI can be used as $\Delta \mathbf{x}_0$ in the implementation system of the method. A larger deformation of the shape can be achieved by accumulating small deformation using Euler integration while eliminating the residual \mathbf{c} by the Newton-Raphson method. Figure 4 shows an example process of design in a design system that can interactively solve Equation 9 while displaying the 3D configuration, flat-folded state, and developed state of the surface. Figure 4 shows an example process of design in a design system that can interactively solve Equation 9 while displaying the 3D configuration, flat-folded state, and developed state of the surface.

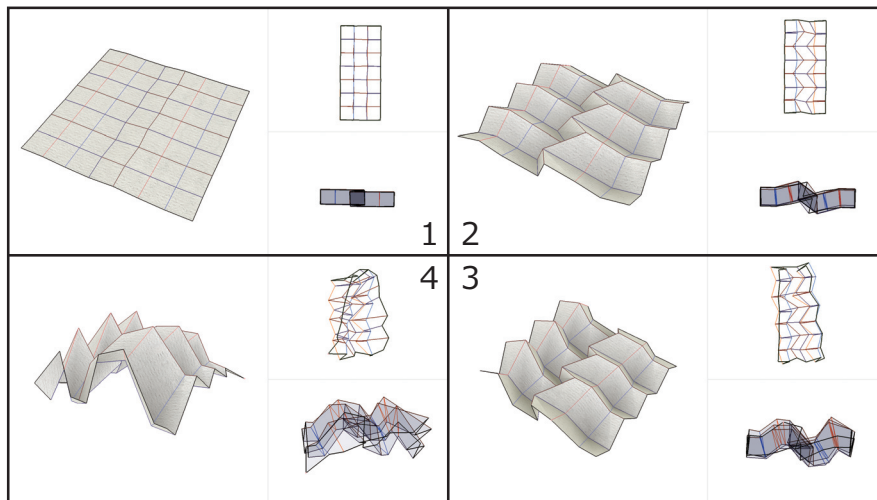


Figure 4: The design process of hybrid pattern obtained by deforming a square grid. Red and dark blue lines indicate mountain and valley foldlines, and pink and light blue indicate complementary mountain and valley foldlines. Each screen shows 3D configuration (left) developed state (upper-right) and flat-foldable shape (lower-right).

The proposed method succeeded in generalizing eggbox pattern and hybrid BDFFPQ mesh. Figure 5 shows an example of a generalized eggbox pattern that has “globally” positive curvature surface, and Figure 6 is an example complex foldable structure based on hybrid surfaces.

4 Rigid Foldable Cylinder

In an architectural context, collapsible cylindrical surfaces are a significant design target since a cylinder qualitatively surrounds a volume of space. Here, note that a cylindrical surface is one of the best possible solutions in this direction since a

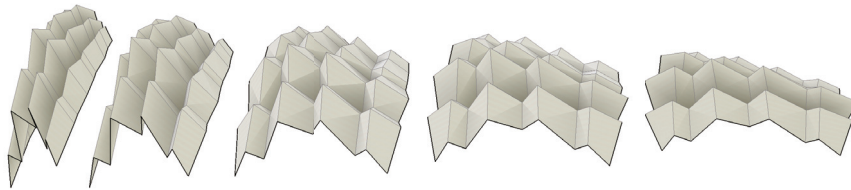


Figure 5: The folding motion of a generalized eggbox pattern.

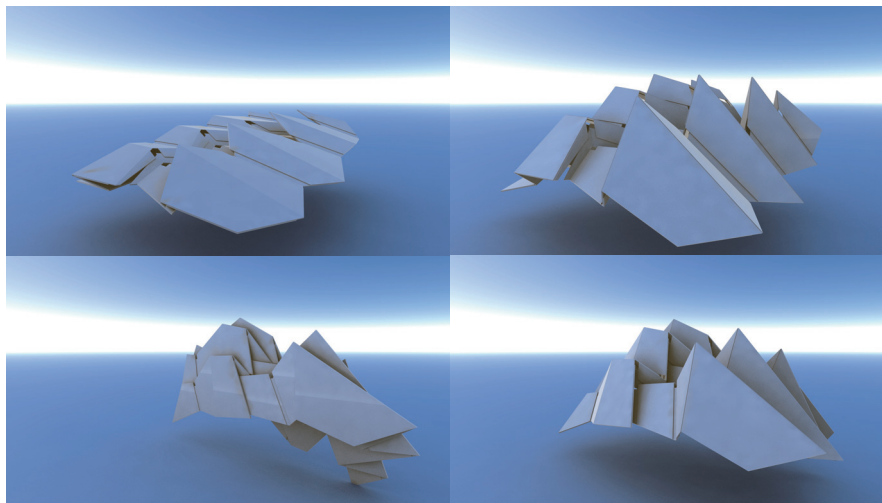


Figure 6: The folding motion of hybrid BDFFPQ mesh.

topologically closed polyhedron, which is ideal in the sense of enclosure of a space, is actually known to forbid a rigid folding motion with volume change as the bellows conjecture [Connelly et al. 1997] states. Although several designs are proposed to enable collapsible and non-rigid-foldable cylinders such as triangulated cylinders [Guest and Pellegrino 1994] and single curved corrugated surface [Hoberman 1993], these exiting designs relied on the flexibility of each facet for the folding motion; they were not applicable to smooth kinetic mechanisms that work with stiff materials and mechanical hinges often required for architectural-scale structures.

[Tachi 2009b] gives a family of cylindrical surfaces and compounds of cylinders that are rigid-foldable and flat-foldable, by solving the angular identity equations via constructing a symmetric modular cylinder based on rotational symmetry and then array copying the obtained module in an axial direction. This successfully produces

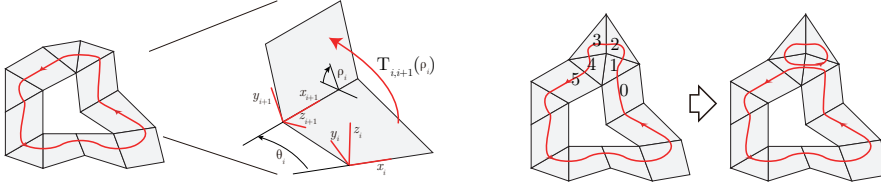


Figure 7: A closed strip of facets (Left). A loop can continuously shrink or expand using conditions around vertices (Right).

a folding motion that does not separate the structure into an open disk. However, the derived surface can only have a constant section along an axis in this approach, and the design variations are limited. Producing freely designed cylindrical surface is the goal of the work described in this section.

The biggest issue in the design of cylindrical surface is that the local condition around each interior vertex is not enough because loops surrounding a hole can geometrically separate by folding; and therefore cylindrical BDFFPQ mesh is not proved to be rigid-foldable in general. In general, it is required that for any closed strip consisting of k facets, the strip does not separate by the folding motion of hinges. We assign a local coordinate to each facet i and denote the local affine transformation from i -th to $i+1$ -th coordinates by 4×4 matrix $\mathbf{T}_{i,i+1}(\{\rho_i\})$ (Figure 7 Left). This transformation is regular and the inverse can be described as $\mathbf{T}_{i,j}^{-1} = \mathbf{T}_{j,i}$. The condition thus is represented as, *there exists a vector function $\rho_i(t)$ ($0 \leq t \leq \pi$) that satisfies the following for any loop of facet strip:*

$$\mathbf{T}_{0,1}\mathbf{T}_{1,2}\cdots\mathbf{T}_{i,i+1}\cdots\mathbf{T}_{k,0} \equiv \mathbf{I}. \quad (10)$$

If the facet fan around each vertex is ensured to be rigid-foldable, loop condition around the vertex modifies the condition along a loop to another homologous loop. For example, in Figure 7 right, the transformation from facet 0 to 5 can be simplified as:

$$\mathbf{T}_{0,1}\mathbf{T}_{1,2}\mathbf{T}_{2,3}\mathbf{T}_{3,4}\mathbf{T}_{4,5} \equiv \mathbf{T}_{0,1}\mathbf{T}_{1,4}\mathbf{T}_{4,5}, \quad (11)$$

using the condition around an interior vertex: $\mathbf{T}_{1,2}\mathbf{T}_{2,3}\mathbf{T}_{3,4}\mathbf{T}_{4,1} \equiv \mathbf{I}$. Therefore, the rigid-foldability of a disk with a hole (or n holes) can be represented by the combination of the local rigid-foldability around each interior vertex and the condition around the hole (or the n -holes).

Since BDFFPQ mesh satisfies local rigid-foldability conditions around vertices, the problem of obtaining a rigid-foldable cylindrical BDFFPQ mesh turns into a problem of obtaining a state with one rigid-foldable loop connected to the surface. We transform an existing rigid-foldable cylinder while ensuring the rigid-foldability of one loop satisfied. In order to do this, we use an isotropic type of rigid-foldable cylinders from [Tachi 2009b] as an initial state, which are symmetrically repeating structures constructed using the combination of degree-4 vertices termed *folds* and

elbows producing a valid loop motion, where a fold and an elbow are symmetric cases of origami vertex and discrete Voss vertex, respectively, in our interpretation. Therefore the cylinder is a symmetric type of rigid-foldable cylindrical BDFFPQ.

Since the exact rigid-foldability condition around a loop is still not fully investigated, we guarantee the rigid-foldability of the whole model by using a sufficient condition: one loop around the hole is unchanged from the original symmetric cylinder. We pick up a strip loop along one of the boundaries that exactly produces a one-DOF motion and rigidify this part using a rigid bar model, while we deform other parts under the local conditions of developability, flat-foldability, and planarity of polygons. The developability and flat-foldability keep the sector angles incident to vertices between rigid strip and flexible BDFFPQ strips fixed and enable a one-DOF motion.

We obtained asymmetric form variations from one symmetric cylindrical structure using the design system that solves BDFFPQ mesh and extra constraints. The design process is shown in Figure 8, and Figure 9 shows the derived crease pattern of the design. The pattern shows the location of foldlines in the developed state (note that the lines are drawn on multiple layers since we use extended definition of developed state). Here, we can notice sets of parallel lines remaining in the generalized pattern. This implies the limitation of our method since this globally symmetric behavior forbids cylinders to change their overall radius; this may restrict the design applications of the cylinders. Since this behavior presumably originates in the fixed boundary of the surface, investigating the exact rigid-foldability condition around a loop and loosening the design constraints can contribute to more flexible designs of rigid-foldable cylinders, which still remains to be a future work.

5 Materialization

Because of the developability of the surface, the structure applied for a small scale object can be manufactured from sheets of material such as paper and plastics. The pattern can be first perforated by cutting plotter, laser cutter, or other CNC 2-axis machines on sheets of thin and hard materials, then pasted together, and folded to form a three-dimensional shape. Careful folding control is needed only at the beginning of the fold; once it is semi-folded, the surface folds automatically since the pattern produces a one-DOF motion. Figure 10 shows a folded model of a rigid-foldable cylinder designed using the proposed method.

For a larger scale architectural structure such as shades, retractable roofs, and transformable partitions, the following thickening method can be used to produce a robust kinetic structure. Each facet is first substituted by two layers of constant thickness panels whose contact plane is the ideal geometric surface. In order to avoid the intersection of panels by the folding motion of $0 \leq \rho_i \leq \pi - \delta_i$ for each foldline, the boundary of the panel in the valley side of the surface is relocated on an offset of the foldline by $t \cot \frac{\delta}{2}$, where t is the thickness of the panel (Figure 11). This yields

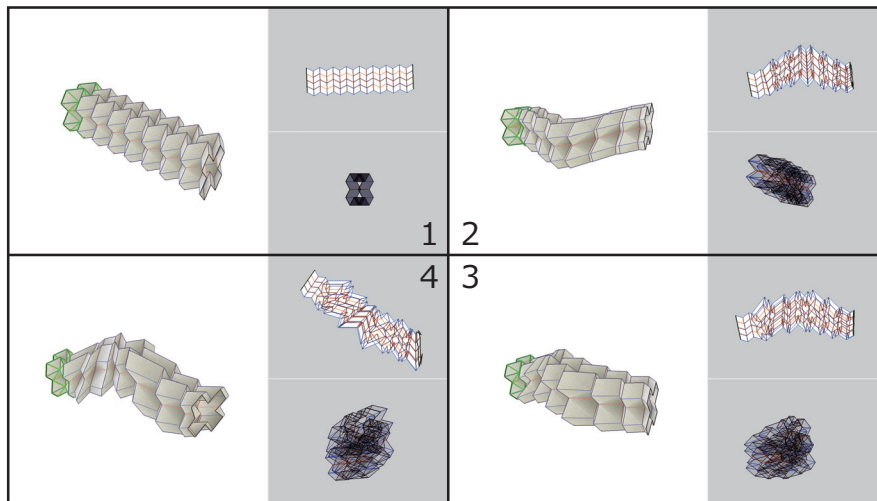


Figure 8: A design process of rigid-foldable cylinder. The initial state is a cylinder by [Tachi 2009b]. The surface is deformed keeping the condition of BDFFPQ mesh while a loop strip (two strips in this redundant case) is maintained to be rigid, as indicated by green rigid bars.

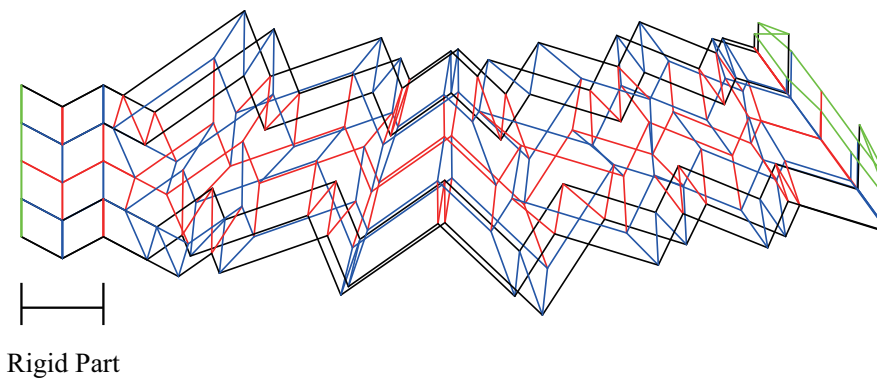


Figure 9: A crease pattern of generalized cylinder.

designs of kinetic structure composed of rigid panels using their edges as rotational hinges as shown in Figures 12 and 13. The hinges can be constructed mechanically or using a sheet or cloth of negligible thickness between panels; in the latter method, the cloth also becomes a watertight covering.

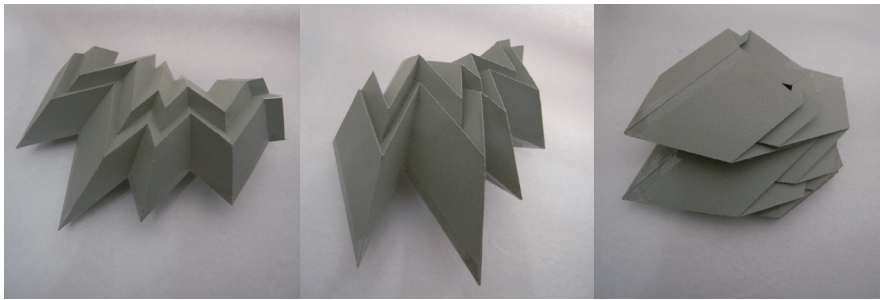


Figure 10: Folded model of a rigid-foldable cylinder. Left: in the developed state, Middle: Intermediate state, Right: flat-folded state.

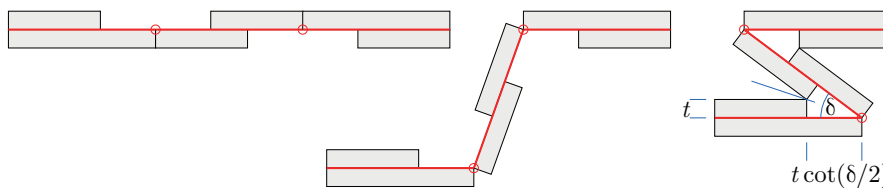


Figure 11: Thickening using two layers of constant thickness panels.

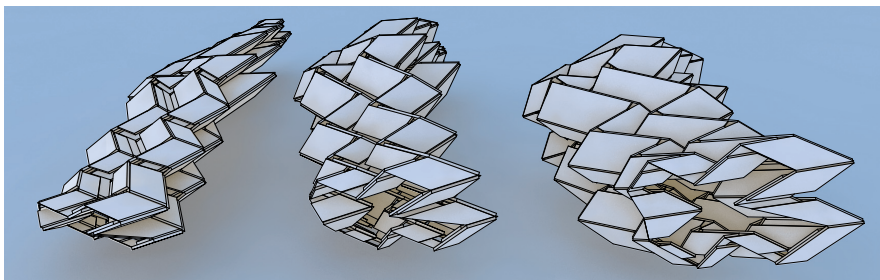


Figure 12: Cylindrical rigid-foldable BDFFPQ mesh consisting of thick panels.

6 Conclusion

In this paper, we presented a design method of rigid-foldable flat-foldable disks and cylinders by introducing bidirectionally flat-foldable planar quadrilateral (BDFFPQ) meshes and their generalization method. The concepts of BDFFPQ mesh, complementary foldlines, and extended definitions of developed and flat-folded states successfully unify and generalize the flat-foldable origami and discrete Voss surfaces. This generalization enables the perturbation based method that can

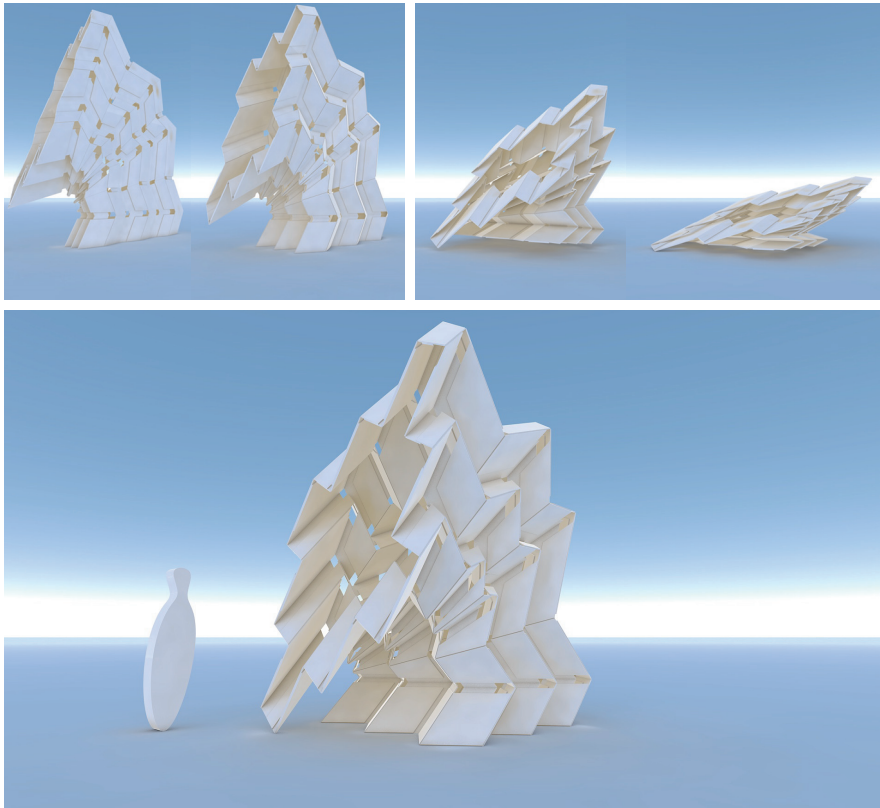


Figure 13: Folding motion of cylindrical structure using thick panels.

freely control the shape of the surface in a direct way; the method yields various designs of rigid-foldable and bidirectionally flat-foldable polyhedral disk. We also investigated the rigid-foldability of a cylindrical surface and its sufficient condition to design a rigid-foldable cylinder. A design method by modifying a cylindrical BDFFPQ mesh with one fixed loop copied from a known rigid-foldable cylindrical structure is introduced. The method enables us to obtain a novel generalized form of rigid-foldable flat-foldable surfaces that can be implemented for architectural design purposes.

It should be noted that we used sufficient condition of the rigid-foldability in this paper and did not provide the exact condition, which still remains to be an unsolved problem as it is seen in [Stachel 2010]. The sufficient condition for enabling cylindrical topology also made the deformation less flexible, the effect of which can be observed in the globally parallel edges. Deriving a more general condition of the rigid-foldability of cylindrical surface and thus enabling a less constrained design is one of the future works of this study.

References

- BRUNNER, A., 1965. Expansible surface structure. United States Patent 3,362,118.
- CONNELLY, R., SABITOV, I., AND WALZ, A. 1997. The bellows conjecture. *Contributions to Algebra and Geometry* 38, 1, 1–10.
- GUEST, S. D., AND PELLEGRINO, S. 1994. The folding of triangulated cylinders, Part I: Geometric considerations. *ASME Journal of Applied Mechanics* 61, 773–777.
- HOBERMAN, C., 1993. Curved pleated sheet structures. United States Patent No. 5,234,727.
- HUFFMAN, D. 1976. Curvature and creases: a primer on paper. *IEEE Transactions on Computers* C-25, 10, 1010–1019.
- MIURA, K. 1980. Method of packaging and deployment of large membranes in space. In *31st Congress of the International Astronautical Federation*.
- SCHIEF, W. K., BOBENKO, A. I., AND HOFFMANN, T. 2007. On the integrability of infinitesimal and finite deformations of polyhedral surfaces. In *Discrete Differential Geometry (Oberwolfach Proceedings)*, 67–93.
- STACHEL, H. 2010. A kinetic approach to Kokotsakis meshes. *Computer Aided Geometric Design*, 27, 428–237.
- TACHI, T. 2009. Generalization of rigid-foldable quadrilateral-mesh origami. *Journal of the International Association for Shell and Spatial Structures* 50, 3 (December), 173–179.
- TACHI, T. 2009. One-DOF cylindrical deployable structures with rigid quadrilateral panels. In *Proceedings of the IASS Symposium 2009*, 2295–2306.
- TACHI, T. 2009. Simulation of rigid origami. In *Origami⁴: The Fourth International Conference on Origami in Science, Mathematics, and Education*, A K Peters, R. Lang, Ed., 175–187.

Authors' address:

Tomohiro Tachi (tachi@idea.c.u-tokyo.ac.jp): The University of Tokyo 3-8-1, Komaba, Meguro-Ku, Tokyo, 153-8902, Japan.